Non-destructive characterization of transparent armor layups

Filipp V. Ignatovich, Kyle J. Hadcock, Donald S. Gibson, Michael A. Marcus

Filipp V. Ignatovich, Kyle J. Hadcock, Donald S. Gibson, Michael A. Marcus, "Non-destructive characterization of transparent armor layups ," Proc. SPIE 10983, Next-Generation Spectroscopic Technologies XII, 109830C (13 May 2019); doi: 10.1117/12.2518724

SPIE.

Event: SPIE Defense + Commercial Sensing, 2019, Baltimore, Maryland, United States

Non-destructive characterization of transparent armor layups

Filipp V. Ignatovich, Kyle J. Hadcock, Donald S. Gibson, Michael A. Marcus
Lumetrics, Inc., 1565 Jefferson Rd #420, Rochester, NY 14623

ABSTRACT

We have developed a material identification instrument, based on measuring the group refractive index dispersion curve using a low-coherence interferometer. Non-destructive product verification testing is critical for multilayer structures used in commercial or military applications. The ability to identify the number of layers in multilayer structures, the material composition of each layer, as well as the thickness of each layer non-destructively is important to ensure product quality in many fields, such as aerospace, defense, automotive and semiconductor. Low-coherence interferometry offers a quick and reliable way of obtaining material dispersion properties by measuring the spectral dependence of the optical thickness of the material. Latest advancements in the supercontinuum light generation have opened new opportunities for these highly accurate spectroscopic measurements. We have successfully applied the developed system to several known and unknown transparent layups.

Keywords: optical dispersion, material identification, transparent armor, low-coherence interferometry, layer thickness

1. INTRODUCTION

Non-destructive product verification testing is a cornerstone for most quality control efforts in manufacturing. It is especially important and challenging for multilayer layup structures, used for a variety of commercial and military applications. Being able to identify the number, thickness and the material of each layer is becoming essential for product verification testing. It may also be used to assess and confirm the properties and capabilities of the layups already deployed for use. Automotive, aerospace, building glazing, transparent armor, compound lenses, semiconductors, displays, and bulletproof glass manufacturing are just some of the example of industries that have the need for non-destructive testing of multilayered structures.

Transparent armor is used in vehicles, aircraft, and buildings to resist enemy fire, vandalism attacks and to protect occupants or valuables within. The United States Department of Defense has been interested in technology that can characterize each layer of a transparent armor window from the strike face through the interior surface. Such technology must identify the material comprising each layer of multi-layer transparent armor layups, including those with closely related materials (e.g. soda lime silica glass versus borosilicate glass, polycarbonate versus polymethyl methacrylate (PMMA), etc.). Along with the thickness of each layer, this information can then be used to describe an overall transparent armor design and make a conclusion about its protective properties.

Transparent armor can be made from various transparent materials (e.g. glasses, plastics, transparent ceramics, and polymer interlayers). The layers of material often range from 0.01 inch thick to over 1 inch thick. Transparent armor window designs can reach over 6 inches in overall thickness and employ dozens of layers of differing materials. Protective properties of the transparent armor depend on the types of the materials, the number of layers, and thicknesses of those layers. It is not possible to visually discern the number, composition, and thickness of each layer when assembled into the end-product, without mechanically cutting a cross-section.

Recently several manufacturers have exited the transparent armor business and some armor products have been left without a supplier. Without reliable non-destructive test method, there is risk in assuming that a deployed armor unit conforms to its intended design and specification. The inspection solution described here allows to reliably test the new and existing transparent armor windows, as installed, to ensure the safety of the military personnel.

Next-Generation Spectroscopic Technologies XII, edited by Richard A. Crocombe, Luisa T. M. Profeta, Abul K. Azad,
Proc. of SPIE Vol. 10983, 109830C · © 2019 SPIE · CCC code: 0277-786X/19/$18 · doi: 10.1117/12.2518724

2. INSTRUMENT DEVELOPMENT

The instrument (ArmorGauge™) is based on a dual free space multi-wavelength Michelson interferometer. It consists of a laser interferometer, and a variable wavelength low-coherence interferometer (LCI). A supercontinuum light source (SCLS) is used for the LCI. During operation, the optical thickness of each layer in multilayer samples is measured with the LCI at a fixed set of distinct center wavelengths by filtering the output of the SCLS with a set of fixed center wavelength narrow bandpass filters.[1] The low coherence interferometer and the laser interferometer share a common variable path length reference arm, and the laser interferometer is used to continuously measure the displacement of the reference path in order to provide an accurate distance scale[2] for the LCI.

Figure 1 shows a schematic of the ArmorGauge™ prototype. Supercontinuum light is directly coupled into a photonic crystal fiber (PCF) which is terminated with a collimator (COL). The SCLS has over 800 mW total power and covers the the spectral range of 450-2400 nm. The collimated supercontinuum light (about 1 mm in diameter) exiting the collimator (COL) passes through a filter wheel (FW) which contains a set of 9 discrete 10 nm bandwidth (≥ OD 4 out-of-band) filters having center wavelengths covering the range of 450 – 750 nm. The specific wavelengths of the filters used in the prototype are 450 nm, 500 nm, 520 nm, 550 nm, 568 nm, 600 nm, 650 nm, 700 nm and 750 nm respectively. The filtered collimated beam is then sent through a polarizing beam splitter (PBS) and a quarter wave plate (QWP) and into the main 50/50 beam splitter cube (BS1) which forms the Michelson interferometer.

The sample and reference beams are focused by the achromatic doublet lenses (LS, LR) on the sample (Sample) and stage reference mirror (MR) respectively. The reference beam achromatic doublet lens and the stage reference mirror are co-mounted on a motorized translation stage (TS) with a maximum of 100 mm travel. The laser interferometer reference mirror ML is also mounted on the translation stage. Light reflected from the reference mirror, and from the sample is recombined by the 50/50 beam splitter into two perpendicular combined beams. The recombined beams are incident onto the two ports of a balanced detector (BD).

The signal from the balanced detector is filtered and amplified. The envelope of the low coherence interferometer signal is then collected as a function of translation stage travel distance (the scan). The use of the balanced detection approach significantly reduces the noise seen by the detector due to removal of common mode noise. Use of balanced detection also enables the ability to use higher SCLS power without saturating the detector.

The schematic of the laser interferometer is shown at the upper portion of Figure 1.

When performing measurements, it is important that the sample is aligned with its surfaces normal to the axis of the incident light from the focusing lens, and at an appropriate depth so that the front optical interface and subsequent optical interfaces in the sample are observed in the interferometer. It is also important to ensure that the location of the focused beam in the sample does not change when switching to different wavelengths. A sample alignment fixture (SAF) has been constructed in order to hold the sample in place. It has both the translational and angular adjustment capabilities to allow the user to optimize alignment of the sample in the interferometer. Figure 2 shows a 12” square layup sample with five layers mounted in the SAF.

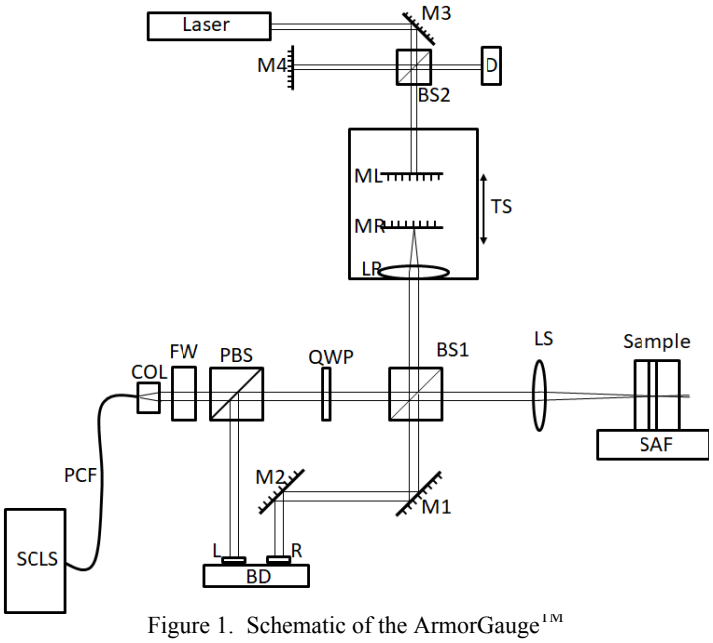

Figure 1. Schematic of the ArmorGauge™

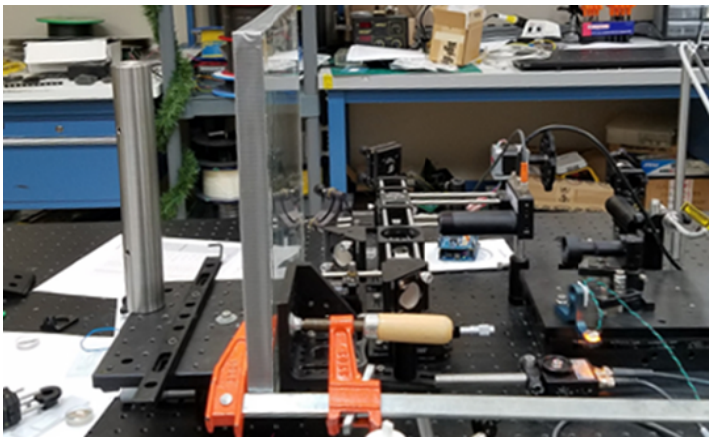

Figure 2. Prototype interferometer shown measuring a 12" square layup having 5 layers

During operation of the interferometer, the translation stage (TS) is repetitively scanned at nearly constant velocity between the opposite end points. One set of measurements is made on all of the layers of the sample during each scan of the translation stage. The scan start location, and the scan velocity of the translation stage are kept the same for all scan. Since the laser has a very long coherence length, the interference in the laser interferometer occurs throughout the scan[1]. The interference in the low coherence interferometer occurs whenever the path distance to the reference mirror is equal in length to an optical interface of the sample, to within a few coherence lengths of the low coherence light source (approximately 20-30 μm). As the translation stage is moved from its start to end position, multiple optical interfaces in the multi-layered sample are observed in the low-coherence interferometric signal.

The interferometric signal data is acquired using National Instruments hardware and software. The LabVIEW interface includes controlling the scan speed and distance, controlling the center wavelength of measurement light, displaying the envelope of the interferometric signal, and acquiring and saving the data. The software accurately determines the locations of each of the interferometric signal peaks as the instrument is scanning and records the optical thickness of each of the observed layers in the sample. The filter wheel is motorized and integrated with the software interface. The software wavelength selector is used to control the filter wheel rotation electronics to place the corresponding filter into the SCLS beam path. Multiple scans (typically a 100) are measured at each wavelength and averaged.

A screenshot of the signal graph in the LabVIEW software interface, corresponding to a 5-layer sample, is shown in Figure 3. The interferometric signal peaks are plotted as a function of the scan distance in real time. The signal peaks correspond to the optical interfaces within the sample. The graphs can be used as an aid in aligning the beam to the sample, by maximizing the amplitudes of the signal peaks before beginning a measurement sequence. The distances between each set of adjacent peaks correspond to measured optical thickness of the corresponding layer.

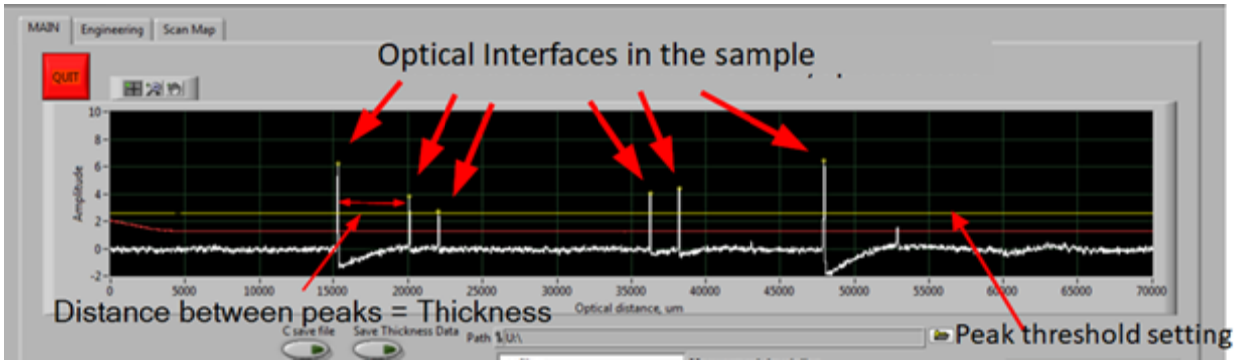

Figure 3. Screenshot of the LabVIEW program interface

3. MATERIAL DISPERSION DATABASE

The phenomenon of optical dispersion is well known for optical materials. The phase velocity $v_p(\lambda)$ of a propagating electromagnetic wave depends on the wavelength of light λ, and so is the phase refractive index:

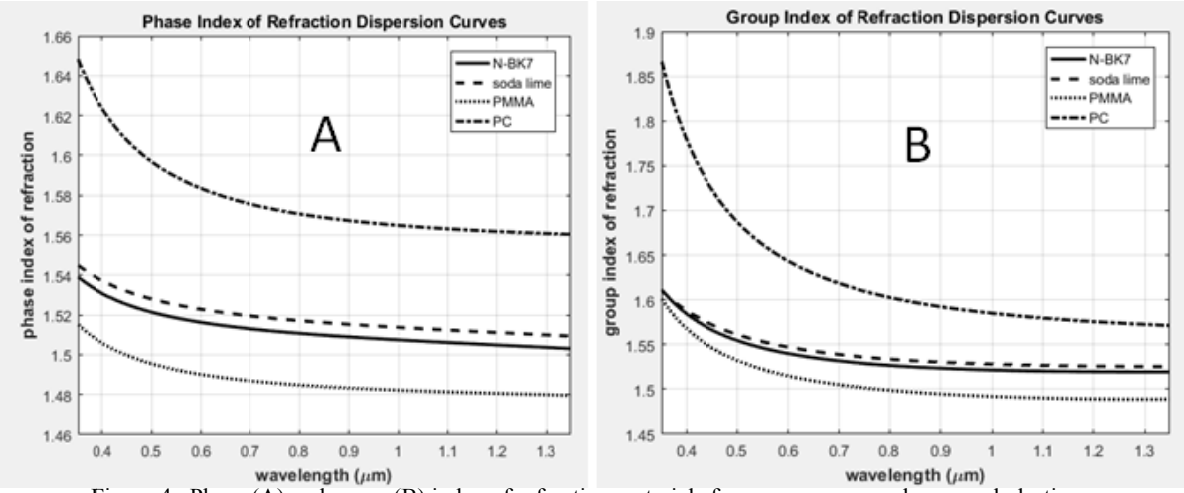

Figure 4. Phase (A) and group (B) index of refraction materials for some common glasses and plastics.

$$n_p(\lambda) = \frac{c}{v_p(\lambda)} \tag{1}$$

where c is the speed of light in vacuum. It has been shown that most optical materials have unique dispersion curves. Instruments for measuring the dispersion curve include spectral ellipsometers, spectral goniometers and refractometers. M. N. Polyanskiy compiled and published an on-line data base of the phase index of refraction dispersion curves for various materials, which can be found online.[3] The online data base also includes the Sellmeier equation coefficients for all of the materials in the database, that can be used to model the dispersion curve using the following equation,

$$n_p^2(\lambda) - 1 = \sum_i^m \frac{B_i \lambda^2}{\lambda^2 - C_i}, \tag{2}$$

where *i* and *m* are integers and *i* varies from 1 to *m*, and B_i and C_i are material dependent constants. For most optical glasses, three sets of coefficients (m = 3) are used and for many plastics only one set (m = 1) is needed.

The group refractive index (GRI) is related to the phase refractive index,

$$n_g(\lambda) = n_p(\lambda) - \lambda \frac{dn_p(\lambda)}{d\lambda} \tag{3}$$

where $dn_p(\lambda)/d\lambda$ is the derivative of the phase index of refraction as a function of wavelength λ. Like in case of the phase index dispersion curve, each material also possesses a unique group index dispersion curve.

Figure 4A shows examples of the phase dispersion curves for soda lime glass, Schott N-BK7 borosilicate glass, polymethyl methacrylate (PMMA) and polycarbonate (PC). Figure 4B shows the calculated GRI dispersion curve for the same set of materials, using data from Polyanskiy. It is usually observed that the GRI is slightly higher than the phase index at a given wavelength, over the wavelength range of 450 - 750 nm.

For the purpose of this work we have created a GRI dispersion database for several materials typically used in the transparent armor. Table 1 shows a sample database containing measured GRIs for six such

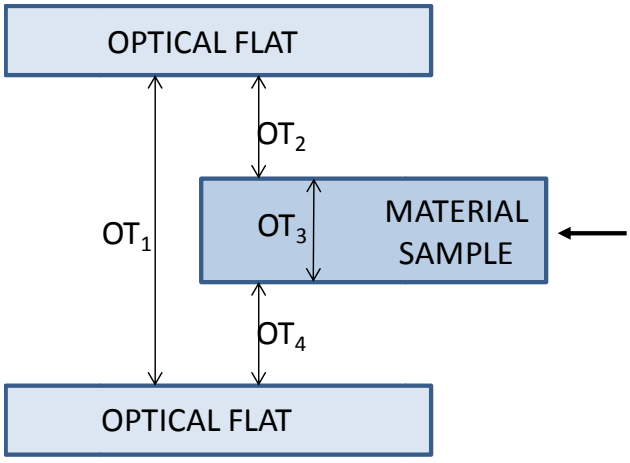

Figure 5. Refractive index measurement chamber schematic.

materials. Single layers of known materials were obtained from vendors. ArmorGauge™ was used to measure the GRI dispersion curves, using a specially constructed index of refraction measurement chamber, as shown in Figure 5. The chamber is composed of a pair of 3 mm thick optical flats mounted in a pair of gimbal mounts. The optical distance between the flats is measured with and then without the test material placed between the flats, at each wavelength. The difference in these two measurements is then used to calculate the GRI.[4]

Table 1. Group index of refraction optical dispersion database.

λ (nm)	Starphire®	PC	Borofloat®33	Plexiglas®	TPU	PVB
450	1.57632	1.71185	1.51521	1.54571	1.55409	1.54010
500	1.56330	1.67654	1.50501	1.53206	1.54057	1.52812
520	1.55884	1.66405	1.50181	1.52761	1.53419	1.52306
550	1.55357	1.64994	1.49766	1.52217	1.52745	1.51776
568	1.55123	1.64390	1.49585	1.51969	1.52589	1.51516
600	1.54702	1.63361	1.49258	1.51541	1.52152	1.51114
650	1.54164	1.62004	1.48848	1.50981	1.51435	1.50520
700	1.53745	1.61002	1.48531	1.50545	1.50994	1.50110
750	1.53413	1.60181	1.48282	1.50196	1.50662	1.49806

4. BEST FIT MATERIAL IDENTIFICATION PROCEDURE

In order to identify the material for 'unknown' layers assembled into a stack, the following procedure was developed. First, using the ArmorGauge™ we acquire the optical thickness of each layer in the layup, at each of the measurement wavelengths. Table 2 shows data obtained from a 3-layer laminate layup sample comprised of nominally 10 mm thick Starphire glass, 1.52 mm thick PVB and 11 mm thick Borofloat 33 glass.

Table 2. Measured optical thickness in μm for each layer in a 3-layer laminate layup

λ (nm)	Layer 1	Layer 2	Layer 3
450	14556.559	2313.334	16928.428
500	14439.139	2295.726	16819.394
520	14395.134	2287.972	16779.671
550	14345.488	2279.946	16733.898
568	14324.352	2275.993	16713.207
600	14286.820	2270.064	16676.923
650	14235.187	2261.316	16628.431
700	14198.418	2254.911	16593.237
750	14166.297	2250.388	16567.469

Second, the measured optical thickness data is compared to the database of known materials. It is done by calculating the physical thickness of each layer using the group refractive index data from the database at each wavelength and for each of material in the database. Such calculation produces a large set of the physical thickness data for each layer. Table 3 shows an example of such data set calculated for the Layer 1 in Table 2.

Table 3. Layer 1 physical thickness test values for known materials in the reference database.

Layer 1 physical thicknesses test						
λ (nm)	Starphire®	PC	Borofloat®33	Plexiglas®	TPU	PVB
450	9234.537	8503.385	9606.930	9417.389	9366.641	9451.687
500	9236.314	8612.474	9594.051	9424.682	9372.588	9448.966
520	9234.497	8650.685	9585.189	9423.284	9382.909	9451.474
550	9233.879	8694.535	9578.571	9424.361	9391.788	9451.75
568	9234.219	8713.632	9576.033	9425.835	9387.545	9453.995
600	9235.074	8745.571	9571.877	9427.688	9389.816	9454.313
650	9233.810	8786.938	9563.561	9428.437	9400.172	9457.357
700	9235.066	8818.794	9559.210	9431.343	9403.305	9458.683
750	9234.121	8843.943	9553.635	9431.901	9402.673	9456.409
Layer 1 statistics						
mean	9234.613	8707.773	9576.562	9426.102	9388.604	9453.848
St. Dev.	0.7836	107.7549	17.0460	4.4448	12.9032	3.1827

The material that results in the most consistent physical thickness at different wavelengths (having the minimum standard deviation) is therefore chosen as the best fit material for that layer. From the bottom row of Table 3 it is immediately clear that the material in Layer 1 of Table 2 is likely the Starphire, and its physical thickness is 9234.6 μm.

Table 4 shows the calculated physical thicknesses and statistics for Layer 2 in Table 2. The second layer is found to be composed of PVB with a thickness of 1502.2 μm. When the best fit material identification procedure is applied to the third layer in Table 2, the best fit material is found to be Borofloat33 with the physical thickness of 11172.9 μm.

Table 4. Calculated physical thickness values for Layer 2 in Table 2 using the GRI database.

Layer 2 thickness test						
λ (nm)	Starphire®	PC	Borofloat®	Plexiglas®	TPU	PVB
450	1467.557	1351.361	1526.737	1496.615	1488.550	1502.066
500	1468.512	1369.325	1525.389	1498.461	1490.178	1502.322
520	1467.737	1374.946	1523.476	1497.743	1491.326	1502.224
550	1467.552	1381.833	1522.334	1497.826	1492.649	1502.179
568	1467.223	1384.507	1521.534	1497.669	1491.585	1502.143
600	1467.381	1389.603	1520.897	1497.986	1491.968	1502.217
650	1466.827	1395.840	1519.209	1497.745	1493.254	1502.339
700	1466.660	1400.550	1518.139	1497.832	1493.379	1502.174
750	1466.887	1404.905	1517.643	1498.305	1493.662	1502.198
Layer 2 thickness statistics						
mean	1467.371	1383.652	1521.707	1497.798	1491.839	1502.207
STD	0.5656	16.7667	3.1337	0.5190	1.6685	0.0842

5. BULLETPROOF GLASS MEASUREMENT EXAMPLE

Figure 6 shows a typical bulletproof glass window with a physical thickness of approximately 4 inches. Measurements were performed with the optical probe first facing the front face and then the back face of the sample. Measurements were made at the 9 different wavelengths and the best fit materials were calculated for each of the measured layers using the previously assembled database.
Figure 7 shows an example of the interferometer scan of 12 layers within the bulletproof glass sample, using center wavelength of 700 nm.

Figure 6. Bulletproof glass sample.

We have asked the supplier of this sample to purposefully introduce errors into the specification sheet. Table 5 summarizes the measurement results. Column 1 shows the layer number, Columns 2 specifies the type of the material, glass or plastic, Column 3 shows the difference between the measured thickness and the specified thickness, Column 4 shows whether we have identified the material as the same as in the specification sheet.

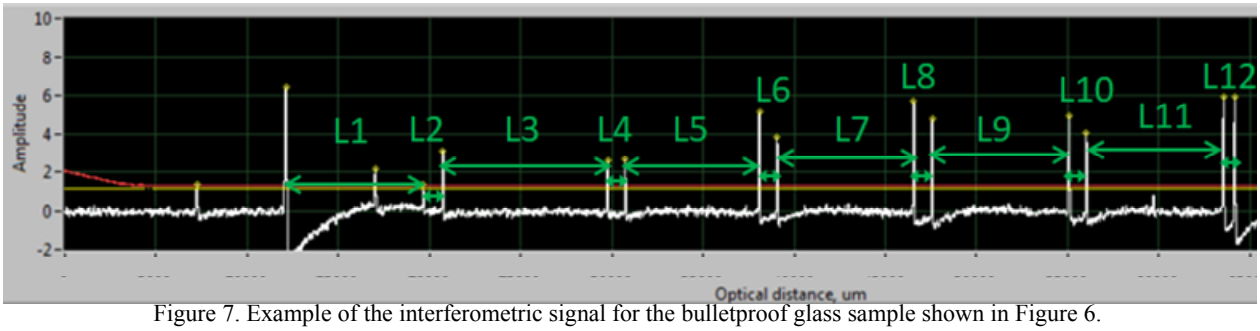

Figure 7. Example of the interferometric signal for the bulletproof glass sample shown in Figure 6.

To preserve trade secrets, we have removed many technical details from the table, such as the exact material make up and thicknesses of most layers, as well as the total number of the layers. However, the table shows that we have successfully identified the material composition and thicknesses of the layers, as well as the purposeful errors in the specification sheet.
The following items can be noted from Table 5:

- Layer #3 is comprised of a low iron soda lime glass (Starphire ®) instead of the Borofloat glass (Borofloat®33);
- Layer #12 is composed of PVB instead of TPU
- We have not measured Layers 13 to N. We have restricted the measurement window to the layers that include outer surfaces. An interferometer with the larger displacement module will be targeted in a later stage of the development to enable measurements of all the layers in a thick sample. Extending the scan depth of the translation stage in our prototype instrument to 250 mm will allow us to measure all the layers of transparent armor up to 150 mm thick from a single side. However, it was not pursued at this preliminary development stage.
- Material for the last layer #(N+9) was not found in our database. We have successfully noted that this is an 'unknown' material and added it to the database. Therefore, the instrument will be able to identify this material again if we encounter it in other samples. In order to accurately measure its thickness, we must also measure it first in the refractive index chamber. At the time of the test measurement of this sample, we did not have data for the GRI in order to accurately determine physical thickness of that layer.

Table 5. Bulletproof glass sample proposed composition, identified materials and layer thicknesses

#	Specified material type	Measured thk minus specified thk, µm	Material identification result
1	GLASS	70	match
2	Plastic	30	match
3	Borofloat33	870	Starphire
4	Plastic	10	match
5	GLASS	-40	match
6	Plastic	30	match
7	GLASS	50	match
8	Plastic	40	match
9	GLASS	70	match
10	Plastic	0	match
11	GLASS	-1430	match
12	TPU	30	PVB
Layers 13 to N were not measured			
N+1	Plastic	20	match
N+2	GLASS	50	match
N+3	Plastic	10	match
N+5	GLASS	-90	match
N+6	Plastic	-10	match
N+7	Plastic	-70	match
N+8	Plastic	-30	match
N+9	Plastic	-300 (approx.)	Not in the database

6. Summary and Conclusions

We have developed a prototype bench-top interferometer (ArmorGauge™) which determines the number of layers, the composition and the thickness of each layer in transparent armor samples. We have found that we can easily distinguish between low iron soda lime silica glass (Starphire), borosilicate glass (Borofloat 33, polycarbonate (PC) and polymethylmethacrylate (Plexiglas), and various interlayer materials including TPU and PVB. The instrument includes a multi-wavelength dual interferometer that measures the optical thickness of each layer in a transparent armor materials sample at multiple wavelengths. Single layer samples of new known materials can be measured by the ArmorGauge™ in a group refractive index measurement cell and added to the materials database.

ACKNOWLEDGMENTS

The authors acknowledge the US Department of Defense for support of this work under the SBIR award contract number W56HZV-18-C-0006.

REFERENCES

[1] Michael A. Marcus, Donald S. Gibson, Kyle J. Hadcock and Filipp V. Ignatovich, "Method of Measurement of Multilayer Structures", US Patent # #10,190,977, January 29, 2019.
[2] Michael A. Marcus, Stanley Gross, "Associated Dual Interferometric Measurement Method for Determining a Physical property of an Object", U.S. Patent # 5,596,409, January 21, 1997.
[3] M. N. Polyanskiy, "Refractive Index Database", https://refractiveindex.info
[4] Marcus, Michael A., Hadcock, Kyle J., Gibson, Donald S., Herbrand, Matthew E. and Ignatovich, Filipp V., "Precision interferometric measurements of refractive index of polymers in air and liquid", Proc. SPIE 8884, Optifab 2013, 88841L (15 October 2013); doi: 10.1117/12.2032533.